and biologically active structures of RNA.[24]

Experimental Section

Materials. Oligonucleotides were synthesized via standard solid-phase cyanoethyl phosphoramidite chemistry on DuPont and Biosearch equipment. The desired sequences were then purified to homogeneity under strongly denaturing conditions (pH 12) using anion-exchange chromatography.[25] The Ni(II) complex **1**, [2,12-dimethyl-2,7,11,17-tetraazabicyclo[11.3.1]heptadeca-1(17),2,11,13,15-pentaene]nickel(II) perchlorate, was synthesized according to published procedures.[26] The terminal oxidant, $KHSO_5$, was obtained from Aldrich. T4 kinase was purchased from BRL, and [γ-^{32}P]ATP (3000 Ci/mmol) was purchased from Amersham. All aqueous solutions were made with purified water (Nanopure, Sybron/Barnsted) and reagents of the highest commercial quality.

Preparation and Reaction of DNA Samples. The concentrations of oligonucleotide stock solutions were calculated from their absorbance at 260 nm and the corresponding ϵ_{260} values estimated from the sum of nucleotide absorptivity as affected by the adjacent bases.[27] The indicated sequences (*) were then labeled at their 5'-terminus with ^{32}P using T4 kinase and [γ-^{32}P]ATP. Duplex structures were annealed by combining each oligonucleotide (3 μM) in a solution of 100 mM NaCl and 10 mM potassium phosphate (pH 7) and then placing this mixture in a water bath heated to 90 °C. After 3 min, the bath was turned off and the samples were allowed to cool along with the bath under ambient conditions (>3 h).

Each nickel-based reaction (100 μL) contained 3 μM of a labeled oligonucleotide (10 nCi), 3 μM **1**, 60 μM $KHSO_5$, 100 mM NaCl, and 10 mM potassium phosphate (pH 7). This mixture was maintained under ambient conditions (except when noted) and quenched after 30 min with 20 mM Na_2SO_3. Samples were then individually dialyzed against 1 mM EDTA pH 8 (2 × 3 h) and water (1 × 12 h), lyophilized, treated with 0.2 M piperidine (60 μL) for 30 min at 90 °C, lyophilized again, and resuspended in 80% formamide containing a 0.1% xylene cyanole and bromophenol blue. Maxam-Gilbert G-specific sequencing reactions were performed by routine protocols.[9] Product fragments of DNA were analyzed by 20% polyacrylamide gel electrophoresis under denaturing conditions (7 M urea) and identified by autoradiography using Kodak X-Omat AR5 film.

Thermal Denaturation of Oligonucleotide Secondary Structure (T_m). Optical melting curves were recorded at 260 nm on a Perkin-Elmer lambda 5 spectrophotometer. Sample solutions were related to those used in the modification studies and contained between ca. 1 and 7 μM total oligonucleotide, 100 mM NaCl, and 10 mM potassium phosphate (pH 7). The T_m values were determined as $^1/_2\Delta A_{260}$.

Acknowledgment. Support of this work through a Seed Grant from the Stony Brook Center for Biotechnology sponsored by the New York State Science and Technology Foundation (to S.E.R. and C.J.B.) and by a grant (to C.J.B.) from the National Science Foundation (CHE-9006684) is gratefully acknowledged. We also thank Prof. Sarah A. Woodson (University of Maryland) for helpful discussions.

Registry No. 1, 35270-39-4; $KHSO_5$, 37222-66-5; guanine, 73-40-5.

(23) (a) Henderson, E.; Hardin, C. C.; Walk, S. K.; Tinoco, I.; Blackburn, E. H. *Cell* **1987**, *51*, 899-908. (b) Sen, D.; Gilbert, W. *Nature* **1988**, *334*, 364-366. (c) Williamson, J. R.; Raghuraman, M. K.; Cech, T. R. *Cell* **1989**, *59*, 871-880. (d) Panyutin, I. G.; Kovalsky, O. I.; Budowsky, E. I.; Dickerson, R. E.; Rikhirev, M. E.; Lipanov, E. E. *Proc. Natl. Acad. Sci. U.S.A.* **1990**, *98*, 867-870.

(24) (a) Jaeger, J. A.; Zuker, M.; Turner, D. H. *Biochemistry* **1990**, *29*, 10147-10158. (b) Woodson. S. A.; Cech, T. R. *Biochemistry* **1991**, *30*, 2042-2050. (c) Perrotta, A. T.; Been, M. D. *Nature* **1991**, *350*, 434-436.

(25) Rokita, S. E.; Romero-Fredes, L. *Biochemistry* **1989**, *28*, 9674-9679.

(26) Karn, J. L.; Busch, D. H. *Nature* **1966**, *211*, 160-162.

(27) Fasman, G., Ed. *Handbook of Biochemistry and Molecular Biology-Nucleic Acids*, 3rd ed; CRC Press: Boca Raton, FL, 1975; p 175.

Mechanistic Studies on the Inhibition of Thermolysin by a Peptide Hydroxamic Acid

Maria Izquierdo-Martin and Ross L. Stein*

Contribution from the Department of Enzymology, R80N-A54, Merck, Sharp, and Dohme Research Laboratories, P.O. Box 2000, Rahway, New Jersey 07065. *Received April 11, 1991*

Abstract: The mechanism of inhibition of thermolysin by the peptide hydroxamic acid HONH-isobutylmalonyl-Ala-GlyNH_2 has been probed by pH and temperature dependencies and solvent deuterium isotope effects. We found the following: (1) At pH 6.5 and 25 °C, the K_i for inhibition of thermolysin by HONH-isobutylmalonyl-Ala-GlyNH_2 is 63 ± 5 nM and reflects a potency for this compound not previously appreciated. (2) The pH dependence of $1/K_i$ at 25 °C is bell-shaped with pK_{a1} = 5.4 ± 0.1, pK_{a2} = 8.2 ± 0.1, and $(K_i)_{limit}$ = 56 ± 4 nM. These pK_a values are similar to those that we obtained from the pH dependence of k_c/K_m for the thermolysin-catalyzed hydrolysis of 3-(2-furyl)acryloyl-Gly-Leu-Ala (hydrolysis at Gly-Leu) and suggest that the active site amino acid residues that are involved in catalysis are also involved in binding this inhibitor. The pH dependence of $1/K_i$ also indicates that thermolysin binds the inhibitor as the neutral, un-ionized acid and not as an anion, as suggested previously by other workers [Holmes, M. A.; Matthews, B. W. *Biochemistry* **1981**, *20*, 6912. Nishino, N.; Powers, J. C. *Biochemistry* **1978**, *17*, 2846. Nishino, N.; Powers, J. C. *Biochemistry* **1979**, *18*, 4340]. (3) At pH 6.5, values of K_i increased with increasing temperature from 18 nM at 5 °C to a plateau of 200 nM between 45 and 60 °C. The van't Hoff plot of this data was analyzed according to a two-step model involving the formation of an initial complex, $(E:I)_1$, that undergoes a conformational isomerization to a second complex, $(E:I)_2$, at high temperature. At temperatures less than 35 °C, only $(E:I)_1$ accumulates and, thus, entirely accounts for inhibition at temperature less than 35 °C. (4) The solvent deuterium isotope effect on K_{ass} ($=K_{ass,H_2O}/K_{ass,D_2O}$, where $K_{ass} = 1/K_i$) is 0.74 ± 0.02 and, like solvent isotope effects for TLN catalysis [$^{D_2O}(k_c/K_m)$ = 0.74; Izquierdo, M.; Stein, R. L. *J. Am. Chem. Soc.* **1990**, *112*, 6054], originates from the transfer of a zinc-bound water molecule to bulk solvent. Based on these results, a mechanism for the inhibition of thermolysin is formulated and discussed.

Introduction

Peptide-derived hydroxamic acids are a class of metalloproteinase inhibitors that are of both medicinal interest, due to the possible involvement of these enzymes in human disease,[1-3] and mechanistic interest, due to insights that might be gained from studying stable complexes of enzymes and these inhibitors.[4-6] The interaction of one of these inhibitors, HONH-benzylmalonyl-L-

(1) Reynolds, J. J. *Brit. J. Dermatol.* **1985**, *112*, 715-723.

(2) Murphy, G.; Gavrilovic, J.; McAlpine, C. In *Proteases in Inflammation and Tumor Invasion*; Tschesche, H., Ed., Walter de Gruyter: Berlin, 1986; pp 173-187.

* To whom correspondence should be addressed.

0002-7863/92/1514-325$03.00/0

Ala-Gly-*p*-nitroanilide, with thermolysin, the prototypical metalloproteinase, has been studied by X-ray crystallography and is seen to involve binding of the peptide portion of the inhibitor to subsites of the extended protease active site and liganding of the hydroxamic acid portion to the active site Zn^{2+}.[6] However, detailed kinetic and mechanistic studies have not been reported for the interaction of a hydroxamic acid with any metalloproteinase.

In this paper, we report pH and temperature dependencies and solvent isotope effects for the inhibition of thermolysin by HONH-Ibm-Ala-GlyNH$_2$.[7] These studies indicate that HONH-Ibm-Ala-GlyNH$_2$ is a potent inhibitor of TLN (K_i = 63 nM; pH 6.5, 25 °C) and suggest that the interaction of this inhibitor with TLN is a complex process involving multiple intermediates.

Materials and Methods

General Procedures. Buffer salts and deuterium oxide were from Sigma Chemical Co. Water was distilled and passed through a deionizer. The TLN substrate, FA-Gly-Leu-Ala, was prepared by Bachem. Buffer solutions for the pH–rate profiles contained 0.01 M $CaCl_2$ and either 0.10 M MES for pHs between 5.0 and 6.5; 0.10 M HEPES for pHs between 6.5 and 8.5; or 0.10 M CHES for pHs between 8.5 and 9.5. Buffers for the solvent isotope effect studies were prepared as described previously.[8,9] Thermolysin was purchased from either Calbiochem or Sigma and prepared as a 3 mg/mL stock solution in pH 7.5 buffer containing 0.10 M HEPES, 0.01 M $CaCl_2$, and 5 M NaBr. The peptide hydroxamic acid, HONH-Ibm-Ala-GlyNH$_2$, was purchased from Calbiochem.

Kinetic Experiments. In a typical kinetic run, 2.89 mL of buffer and 0.100 mL of substrate, FA-Gly-Leu-Ala, in DMSO were added to a 3-mL cuvette, and the cuvette was placed in the jacketed cell holder of an Aviv Model 14DS spectrophotometer. Temperature was maintained by water circulated from a Brinkman RM6 water bath. Using an Omega thermistor thermometer, we continuously monitored the temperature of a water-filled cuvette that was placed in a position of the cell holder directly adjacent to the reaction solution. Temperature variation during a kinetic run was less than ±0.02 °C. After the reaction solution had reached thermal equilibrium (>15 min), we initiated the reaction by the addition of 0.010 mL of enzyme stock solution. Reaction progress was monitored by the absorbance change at 322 nm ($\Delta\epsilon$ = −2300) that accompanies cleavage of FA-Gly-Leu-Ala at the Gly–Leu bond. For each kinetic run, between 600 and 1000 data points, corresponding to {time, OD_{322}} pairs, were collected by an AT&T, PC 6300 microcomputer interfaced to the spectrophotometer. Since these reactions were all done under the condition that [S] ≪ K_m, the progress curves were first-order in substrate and were fit to a simple first-order rate law. The analysis program was written by Dr. Phil Huskey (Chemistry Department, Rutgers University, Newark, NJ).

Determination of K_i Values for pH- and Temperature-Dependence Studies. For each set of experimental conditions, a K_i value was calculated at a single concentration of inhibitor according to the expression

$$K_i = \frac{[I]}{\frac{k_0}{k_i} - 1} \qquad (1)$$

where k_0 and k_i are pseudo-first-order rate constants determined at subsaturating concentrations of substrate for the hydrolysis FA-Gly-Leu-Ala in the absence and presence of inhibitor, respectively. In these experiments, $[E]_0$ = 0.010–0.054 μM, $[I]_0$ = 0.11–1.1 μM, and $[S]_0$ = 10 μM. Since substrate concentration was at least 10-fold less than K_m, the K_i that we calculate from eq 1 is a true, competitive dissociation constant and, thus, reflects dissociation of the most stable enzyme:inhibitor complex.

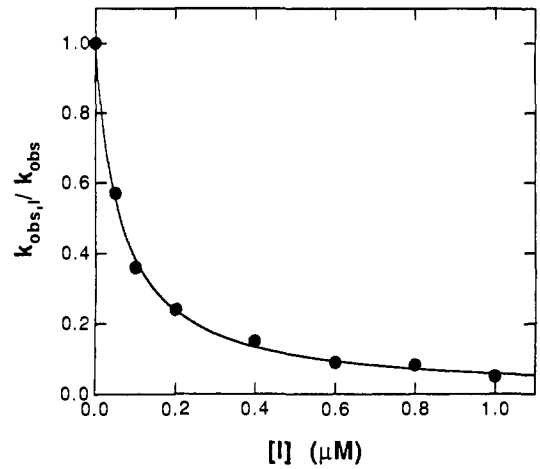

Figure 1. Inhibition of TLN by HONH-Ibm-Ala-GlyNH$_2$. Pseudo-first-order rate constants, k_{obs}, were determined for the TLN-catalyzed hydrolysis of FA-Gly-Leu-Ala in the absence and presence of various concentrations of the hydroxamic acid inhibitor, HONH-Ibm-Ala-GlyNH$_2$ ($[E]_0$ = 0.022 μM, $[S]_0$ = 10 μM; pH 6.5, 25 °C). In this figure, the normalized quantity, $k_{obs,I}/k_{obs}$ is plotted vs [I] and fit to the simple equation $k_{obs,I}/k_{obs} = 1/(1 + [I]/K_i)$ to arrive at the best fit value: K_i = 0.062 ± 0.002 μM. This equation and K_i value were used to draw the line through the points.

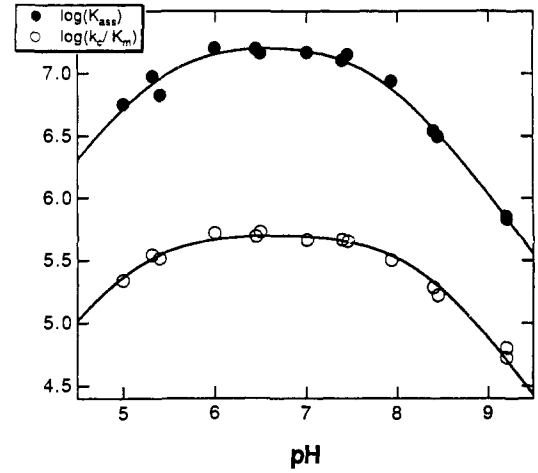

Figure 2. pH dependence of log (k_c/K_m) for the TLN-catalyzed hydrolysis of FA-Gly-Leu-Ala and log K_{ass} for the inhibition of TLN by HONH-Ibm-Ala-GlyNH$_2$. Reactions were run at 25 °C in buffer solutions containing 0.01 M $CaCl_2$ and either 0.10 M MES for pHs between 5.0 and 6.5; 0.10 M HEPES for pHs between 6.5 and 8.5; or 0.10 M CHES for pHs between 8.5 and 9.5. The theoretical lines were drawn using the logarithmic transform of eq 2 and the best fit parameters $(k_c/K_m)_{limit}$ = 525 000 M^{-1} s^{-1}, pK_{a1} = 5.11, and pK_{a2} = 8.23 for k_c/K_m and $(K_{ass})_{limit}$ = 1.79 × 10^7 M^{-1}, pK_{a1} = 5.39, and pK_{a2} = 7.81 for K_{ass}.

Results

Inhibition of Thermolysin by HONH-Ibm-Ala-GlyNH$_2$. From triplicate experiments of the sort illustrated in Figure 1, we calculate a K_i of 63 ± 5 nM for the inhibition of TLN by HONH-Ibm-Ala-GlyNH$_2$ at pH 6.5 and a temperature of 25 °C. This inhibitor is nearly 1 order of magnitude more potent than previously reported. Nishino and Powers[4,5] estimated that the K_i of this inhibitor is near 480 nM, not the 60 nM that we observe. Their underestimate of potency is undoubtedly due to their use of a high thermolysin concentration of about 420 nM.[4,5]

pH Dependence of Thermolysin Catalysis and Inhibition. Values of k_c/K_m for the TLN-catalyzed hydrolysis of FA-Gly-Leu-Ala and K_i for the inhibition of TLN by HONH-Ibm-Ala-GlyNH$_2$ were determined at several pH values between 5 and 10 and are presented in Figure 2 as plots of log (k_c/K_m) vs pH and log K_{ass} vs pH where K_{ass} is the association equilibrium constant for enzyme and inhibitor and is equal to $(K_i)^{-1}$.

(3) Khokha, R.; Denhardt, D. T. *Invasion Metastasis* **1989**, *9*, 391–405.
(4) Nishino, N.; Powers, J. C. *Biochemistry* **1978**, *17*, 2846–2850.
(5) Nishino, N.; Powers, J. C. *Biochemistry* **1979**, *18*, 4340–4347.
(6) Holmes, M. A.; Matthews, B. W. *Biochemistry* **1981**, *20*, 6912–6920.
(7) Abbreviations: FA, 3-(2-furyl)acryloyl; Mns, 6-(*N*-methylanilin)-2-naphthylene-1-sulfonyl; Z, carbobenzoxoyl; Ibm, isobutylmalonyl, –COCH(CH$_2$CH(CH$_3$)$_2$)CO–; Nva, norvaline; TLN, thermolysin; eu, entropy unit (cal/mol·K).
(8) Stein, R. L.; Elrod, J. P.; Schowen, R. L. *J. Am. Chem. Soc.* **1983**, *105*, 2446–2452.
(9) Stein, R. L.; Strimpler, A. M.; Hori, H.; Powers, J. C. *Biochemistry* **1987**, *26*, 1305–1314.

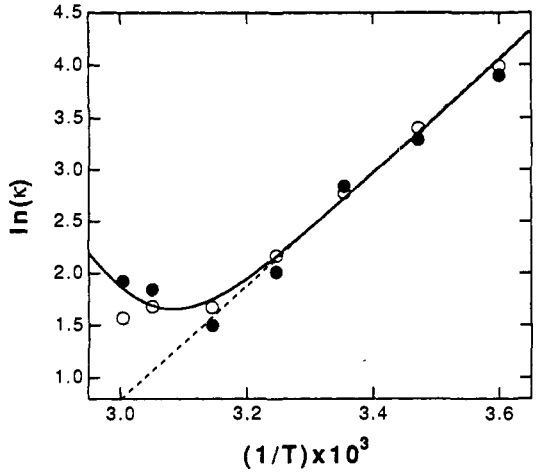

Figure 3. van't Hoff plot for the inhibition of TLN by HONH-Ibm-Ala-GlyNH$_2$. $\kappa = K_{ass}[I]_{std\ state}$, where $[I]_{std\ state} = 10^{-6}$ M. Reactions were run in a pH 6.48 buffer containing 100 mM MES and 10 mM $CaCl_2$. The filled and empty circles represent the results of two independent experiments. In the experiment represented by the filled circles, [E] = 10 nM and [I] = 80 nM, while in the experiment represented by the empty circles [E] = 10 nM and the inhibitor was increased with increasing temperature so that the rate constant in the presence of inhibitor was about half the control rate constant. The solid, curved line was drawn using eq 5 and the nonlinear least-squares best fit parameters $\Delta H_1 = -10.9$ kcal/mol, $\Delta S_1 = -31.2$ eu, $\Delta H_2 = 32$ kcal/mol, and $\Delta S_2 = 97$ eu. The dashed, straight line represents the temperature dependence for a simple, one-step mechanism and was drawn using the equation $\kappa = \exp(-\frac{\Delta H_1}{RT} + \frac{\Delta S_1}{R})$ with $\Delta H_1 = -10.9$ kcal/mol and $\Delta S_1 = -31.2$ eu.

Both curves are bell-shaped with plateaus of activity around pH 6. The general expression of eq 2 was used to fit the data.

$$k_{obs} = \frac{k_{limit}}{1 + \frac{[H^+]}{K_{a1}} + \frac{K_{a2}}{[H^+]}} \quad (2)$$

In this equation, K_{a1} and K_{a2} are acid dissociation constants for amino acid residues of the free enzyme that are important for catalysis and inhibition. For k_c/K_m, the following best fit parameters were obtained: $(k_c/K_m)_{limit} = (5.25 \pm 0.25) \times 10^5$ M^{-1} s^{-1}; p$K_{a1} = 5.11 \pm 0.09$; p$K_{a2} = 8.23 \pm 0.05$. For K_i the following were obtained: $(K_i)_{limit} = 56 \pm 4$ nM; p$K_{a1} = 5.39 \pm 0.08$; p$K_{a2} = 7.81 \pm 0.06$.

From literature determinations of the pH dependencies of substrate hydrolysis,[10,11] we can calculate the average values: p$K_{a1} = 5.1 \pm 0.1$ and p$K_{a2} = 8.2 \pm 0.1$. From the results of this study, we see that the pK_{a1} values that we determined from the pH dependencies of log (k_c/K_m) and log K_{ass} as well as the pK_{a2} value that we determined for the pH dependence of log (k_c/K_m) compare favorably with literature. However, the pK_{a2} value that we determined from the pH dependence of log K_{ass} is lower than the literature average by about 0.4 pH unit. While this difference is statistically significant, it is unclear if it is mechanistically significant.

Temperature Dependence for the Inhibition of Thermolysin by HONH-Ibm-Ala-GlyNH$_2$. Values of K_i for the inhibition of TLN by HONH-Ibm-Ala-GlyNH$_2$ were determined at seven temperatures from 5 to 60 °C and were used to construct the van't Hoff plot of Figure 3. For this plot, values of K_{ass} were first multiplied by a standard-state inhibitor concentration of 10^{-6} M to provide the unitless equilibrium constant κ.

The van't Hoff plot of Figure 3 is clearly nonlinear and indicates that the association of HONH-Ibm-Ala-GlyNH$_2$ with TLN is not a simple one-step process. Although a number of mechanisms can account for such curvature,[12] the simplest of these that is consistent with all of our data is shown in Scheme I. In this scheme, K_1 is a unitless association constant that is equal to $[I]_{std\ state}/K_{i,1}$, where $K_{i,1}$ is the dissociation constant for $(E:I)_1$, and K_2 is an equilibrium constant. For the mechanism of Scheme I

$$\kappa = K_1(1 + K_2) \quad (3)$$

or if we express K_1 and K_2 in their thermodynamic forms

$$\kappa = [\exp(-\Delta G_1/RT)][1 + \exp(-\Delta G_2/RT)] \quad (4)$$

Replacing ΔG with $\Delta H - T\Delta S$, eq 4 becomes

$$\kappa = \left\{\exp\left(-\frac{\Delta H_1}{RT} + \frac{\Delta S_1}{R}\right)\right\}\left\{1 + \exp\left(-\frac{\Delta H_2}{RT} + \frac{\Delta S_2}{R}\right)\right\} \quad (5)$$

Fitting the data of Figure 3 to eq 5 by nonlinear least-squares analysis provides the following estimates for the thermodynamic parameters: $\Delta H_1 = -10.9 \pm 0.8$ kcal/mol, $\Delta S_1 = -31.2 \pm 2.9$, $\Delta H_2 = 32 \pm 9$ kcal/mol, and $\Delta S_2 = 97 \pm 26$ eu. The latter two parameters are poorly defined due to the few number of data points at temperatures above 50 °C.

At temperatures below about 35 °C, κ is controlled by K_1 and $(E:I)_2$ does not accumulate to any significant amount. This is illustrated in Figure 4 where we have plotted the temperature dependence of the distribution of the three enzyme forms of Scheme I. The theoretical curves were drawn using the thermodynamic parameters given in the previous paragraph and the relationships

$$\frac{[E]}{[E]_{total}} = \frac{1}{1 + \kappa} \quad (6)$$

$$\frac{[(E:I)_1 + (E:I)_2]}{[E]_{total}} = \frac{\kappa}{1 + \kappa} \quad (7)$$

$$\frac{[(E:I)_1]}{[E]_{total}} = \frac{K_1}{1 + \kappa} \quad (8)$$

$$\frac{[(E:I)_2]}{[E]_{total}} = \frac{K_1K_2}{1 + \kappa} \quad (9)$$

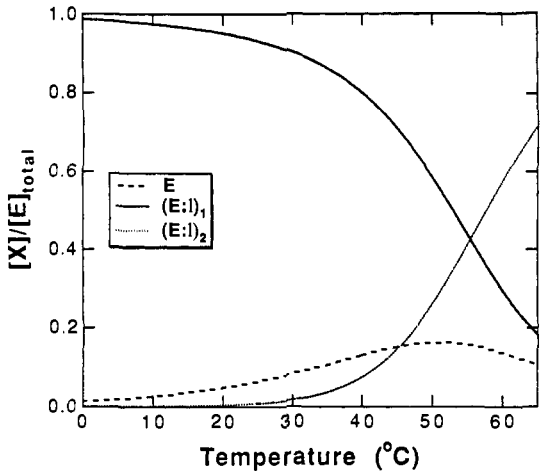

Figure 4. Distribution of enzyme forms according to the mechanism of Scheme I for the inhibition of TLN by HONH-Ibm-Ala-GlyNH$_2$. $[I]_{std\ state} = 10^{-6}$ M. See text for details.

Scheme I. Proposed Mechanism for the Inhibition of TLN by HONH-Ibm-Ala-GlyNH$_2$

$$E \underset{}{\overset{K_1}{\rightleftharpoons}} (E:I)_1 \overset{K_2}{\rightleftharpoons} (E:I)_2$$

(10) Fukuda, M.; Kunugi, S. *Bull. Chem. Soc. Jpn.* **1984**, *57*, 2965–2970.
(11) Kunugi, S.; Hirohara, H.; Ise, N. *Eur. J. Biochem.* **1982**, *124*, 157–163.
(12) Izquierdo, M.; Stein, R. L. *J. Am. Chem. Soc.* **1990**, *112*, 6054–6062.

Table I. Summary of Mechanistic Probes for the Inhibition of TLN by HONH-Ibm-Ala-GlyNH_2

mechanistic probe	result
pH dependence of k_c/K_m	$(k_c/K_m)_{limit}$ = 525 000 ± 25 000 M^{-1} s^{-1}
	pK_{a1} = 5.11 ± 0.09
	pK_{a2} = 8.23 ± 0.05
pH dependence of K_i	$(K_i)_{limit}$ = 56 ± 4 nM
	pK_{a1} = 5.39 ± 0.08
	pK_{a2} = 7.81 ± 0.06
temperature dependence	curved; suggests the two-step mechanism of Scheme I
	ΔH_1 = −11 ± 1 kcal/mol
	ΔS_1 = −31 ± 3 eu
	ΔH_2 = 32 ± 9 kcal/mol
	ΔS_2 = 97 ± 26 eu
solvent isotope effect	$^{D_2O}(K_{ass})$ = 0.74 ± 0.02
	independent of temperature

Scheme II. General Ionization Scheme for Thermolysin

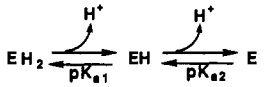

Only above 35 °C does K_2 significantly affect the magnitude of K.

Solvent Deuterium Isotope Effects on K_{ass}. Solvent deuterium isotope effects on K_{ass} (expressed as the ratio of K_{ass} in H_2O to K_{ass} in D_2O and abbreviated as $^{D_2O}(K_{ass})$) were determined for the inhibition of TLN by HONH-Ibm-Ala-GlyNH_2 as a function of temperature. At 5, 25, and 55 °C, $^{D_2O}(K_{ass})$ equals 0.73 ± 0.07, 0.74 ± 0.04, and 0.76 ± 0.02, respectively. These values are insensitive to temperature and are identical to $^{D_2O}(k_c/K_m)$ for the TLN-catalyzed hydrolyses of FA-Gly-Leu-Ala and FA-Gly-LeuNH_2.[12,13]

Determination of the pK_a of HONH-Ibm-Ala-GlyNH_2. A 1.1 mM solution of HONH-Ibm-Ala-GlyNH_2 was titrated with 10 mM NaOH on a Radiometer PHM 84 Research pH meter equipped with a combination electrode. The inflection point, or pK_a, for the resultant titration curve is 8.78. This value is similar to the pK_a of 9.37 for acetohydroxamic acid.[14]

Discussion

The goal of this study was to probe the mechanism of inhibition of thermolysin by the peptide hydroxamic acid HONH-Ibm-Ala-GlyNH_2. To this end, we employed three probes of mechanism: pH and temperature dependencies and the solvent deuterium isotope effect. The results of these studies are summarized in Table I. In this section, we will first discuss these results individually and then attempt to integrate them into an internally consistent picture for thermolysin catalysis and inhibition.

pH Dependence of Catalysis and Inhibition. In this study, we confirmed experimental results reported by several laboratories[10,11] for the pH dependence of k_c/K_m for reactions of thermolysin. The pH dependence that we observe for k_c/K_m is bell-shaped with pK_a values of 5.1 and 8.2. Since these pK_a values were derived from the pH dependence of k_c/K_m, they reflect the ionization of catalytically essential groups of either free enzyme or substrate. We believe that both of these values reflect ionization of enzyme and not substrate since the same pK_a values are obtained for non-ionizing substrates such as FA-Gly-LeuNH_2.[11]

The general ionization scheme that the pH dependence of k_c/K_m suggests is shown in Scheme II, where the active form of the enzyme is EH. The assignment of these pK_a values to active site residues is still a matter of debate, however. Three hypotheses for active site ionization are illustrated in Scheme III.

Scheme IIIA reflects a conventional interpretation[10,11] in which the pK_a near 5 reflects ionization of the active site pair {Glu_{143}-COOH H_2O-ZnL_3} to {Glu_{143}-COO··H··O(H)-ZnL_3},

Scheme III. Active Site Ionizations for Thermolysin

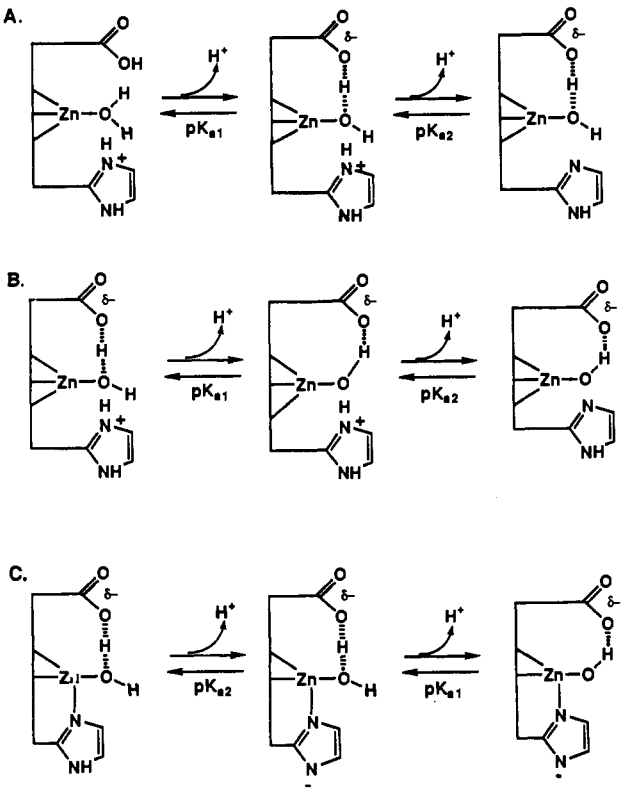

where L_3 are the three zinc ligands, His_{142}, His_{146}, and Glu_{166}. There is, of course, no way to know if the departing proton comes from Glu_{143}-COOH or H_2O-ZnL_3. Also, according to Scheme IIIA, the ionization with pK_a 8 corresponds to His_{231}-ImH^+.

The second proposal, shown in Scheme IIIB, states the pK_a of 5 corresponds to the ionization of {Glu_{143}-COO··H··O(H)-ZnL_3} to {Glu_{143}-COO··H··O-ZnL_3}. This not an unreasonable assignment since metal-bound water molecules are known to have pK_a values that are much less than 14 and, in fact, similar assignments have been suggested for several other zinc-dependent enzymes.[15-18] We again assign the pK_a of 8 to ionization of His_{231}-ImH^+.

Finally, in Scheme IIIC, is a proposal advanced by Mock and Tsay for carboxypeptidase A.[16,17] In this proposal, the low pK_a again corresponds to ionization of {Glu_{143}-COO··H··O(H)-ZnL_3} to {Glu_{143}-COO··H··O-ZnL_3}, but now the high pK_a corresponds to ionization of one of the two histidine residues, His_{142} or His_{146}, that serve as ligands to the zinc to an imidazole anion. In this case the active form of the enzyme at neutral pH is the minor form: Glu_{143}-COO··H··O(H)-ZnL_2-Im^--His. However, the mechanism for peptide bond hydrolysis in which this enzyme form would participate is not clear.

We have chosen to interpret the pH dependencies of k_c/K_m and K_{ass} in the context of Scheme IIIA. An important feature of this ionization scheme is the involvement a zinc-bound water rather than a zinc-bound hydroxide since as we argue below, only the water molecule, and not the tightly bound hydroxide, can be displaced from zinc by the inhibitor.[16,17] Furthermore, it is not yet clear that ionization of the imidazole of a histidine zinc ligand is general and can be extended to metalloproteinases other than carboxypeptidase A. Thus, we chose to interpret our data in the context of the simplest ionization scheme; that of Scheme IIIA.

The mechanism that we propose for thermolysin-catalyzed peptide hydrolysis, and the one that will form the interpretational

(13) Stein, R. L. *J. Am. Chem. Soc.* **1988**, *110*, 7907-7908.
(14) Schwarzenbach, G.; Schwarzenbach, K. *Helv. Chim. Acta* **1963**, *46*, 1390-1400.
(15) Kassebaum, J. W.; Silverman, D. N. *J. Am. Chem. Soc.* **1989**, *111*, 2691-2696.
(16) Mock, W. L.; Tsay, J.-T. *Biochemistry* **1986**, *25*, 2920-2927.
(17) Mock, W. L.; Tsay, J.-T. *J. Biol. Chem.* **1988**, *263*, 8635-8641.
(18) Schmidt, J.; Chen, J.; DeTraglia, M.; Minkel, D.; McFarland, J. T. *J. Am. Chem. Soc.* **1979**, *101*, 3634-3640.

Scheme IV. Chemical Mechanisms for Thermolysin Catalysis and Inhibition

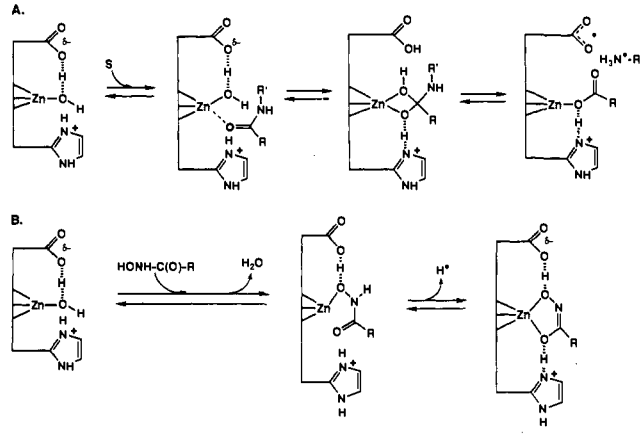

foundation for the inhibition data, is shown in Scheme IVA. This mechanism contains important features that were previously suggested by both crystallographic and modeling studies.[6,19,22]

In the first step of the mechanism Scheme IVA, enzyme and substrate combine to form a Michaelis complex in which the carbonyl oxygen of the substrate forms the fifth ligand to the zinc and displaces the bound water toward Glu_{143}. In the second step of the reaction, the zinc-bound water attacks the carbonyl carbon to form a tetrahedral intermediate. We propose that this step occurs with protolytic assistance by Glu_{143}. The tetrahedral intermediate that forms as a consequence of this attack, as well as the transition state leading to this intermediate, are stabilized by a hydrogen bond from His_{231}-ImH^+. As we learned from the pH dependence of k_c/K_m and Scheme II, this is an essential role for His_{231} since deprotonation of His_{231}-ImH^+ (EH) to His_{231}-Im (E) is accompanied by a loss of enzyme activity. Finally, the tetrahedral intermediate collapses to form product amine and zinc-bound carboxylate which is again stabilized by a hydrogen bond from His_{231}-ImH^+. Protonation of the amine leaving group occurs by either Glu_{143}-COOH or a solvent water molecule. This contrasts with previous suggestions[10,11] that leaving group protonation is by His_{231}. Crystallographic results[6,21,22] suggest that His_{231} is too remote to act as the proton donor during the collapse of the tetrahedral intermediates.

With the mechanism for thermolysin catalysis as our foundation, we now construct a mechanism for the inhibition of thermolysin by HONH-Ibm-Ala-GlyNH_2 (see Scheme IVB). In the first step, the hydroxamic acid binds to the enzyme with elimination of water to yield a monodentate complex with the active site zinc. The displacement of water probably does not occur in a single step as we show it here, however, but rather probably involves the initial formation of a simple Michaelis complex from which water displacement by inhibitor occurs. A preassociative mechanism such as this does not require the energetically unfavorable departure of water from the active site zinc prior to entry of the inhibitor.

In the second and final step of the mechanism of Scheme IVB, we propose that the hydroxamic acid ionizes to its anionic form to allow the formation of the stable, bidentate complex that is observed crystallographically.[6] Once formed at the active site of thermolysin, the anion is stabilized by hydrogen bonds to both Glu_{143}-COO^- and His_{231}-ImH^+.[6] This explains the pH dependence of K_{ass} which requires Glu_{143} and His_{231} to be in these ionization states. It is important to stress that there is no evidence that *requires* the hydroxamic acid to ionize at the active site. We

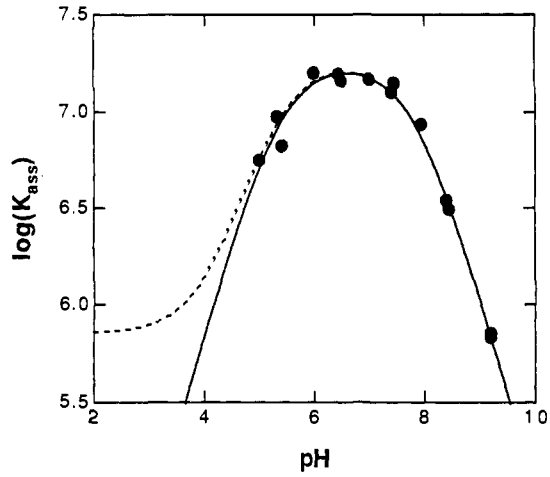

Figure 5. pH dependence of inhibition according to the simple ionization Scheme II (solid line; drawn using eq 2 with pK_{a1} = 5.39 and pK_{a2} = 7.81) and a more complex ionization scheme in which the bound hydroxamic acid also dissociates (dashed line; drawn using eq 10 with pK_{a1} = 5.39, pK_{a2} = 7.81, and pK_{a3} = 4).

propose it based on known chemistry of complex formation between hydroxamic acids and metals in which cases it is the hydroxamate anion and not the acid that binds metals tightly.[23]

Now, the pH dependence of K_{ass} for the mechanism we just described is not adequately expressed by eq 2, but rather requires the slightly more complex expression of eq 10 which takes into account ionization of the enzyme-bound hydroxamic acid. In

$$(K_{ass})_{obs} = (K_{ass})_{limit}\left\{\frac{1 + \frac{[H^+]}{K_{a3}}}{1 + \frac{[H^+]}{K_{a1}} + \frac{K_{a2}}{[H^+]}}\right\} \qquad (10)$$

this equation, K_{a1} again refers to ionization of the active site pair {Glu_{143}-COOH H_2O-ZnL_3} to {Glu_{143}-COO^-···H···O(H)-ZnL_3}. Binding of inhibitor to the un-ionized pair is unfavorable since this would not allow hydrogen bonding of the inhibitor to Glu_{143}-COO^-, while further ionization is unfavorable since this would not allow displacement of the zinc-bound hydroxide that this ionization would form.[16,17] K_{a2} refers to ionization of His_{231}-ImH^+ which is required to allow stabilization of the final anionic complex. Finally, K_{a3} is the pK_a of the zinc-bound inhibitor. Although we do not know the magnitude of K_{a3}, it is not unreasonable to expect that, like water, the zinc-bound hydroxamic acid would become more acidic and experience a decrease in pK_a. And, in fact, as we illustrate in Figure 5, if the pK_a of the enzyme-bound hydroxamic acid is less than 4, its ionization would be kinetically invisible in the pH range of our experiments. Since the pK_a of HONH-Ibm-Ala-GlyNH_2 is 8.8, a stabilization to a pK_a of 4 on the enzyme is reasonable since it is smaller than the pK_a perturbation that water experiences.

The mechanism that we propose in Scheme IVB contrasts with a previously proposed mechanism[4-6] which states that it is the ionized form of the hydroxamic acid that binds to thermolysin. Our data are inconsistent with this view. If inhibition was dependent on the binding of the anionic form of HONH-Ibm-Ala-GlyNH_2, K_{ass} would increase with increasing pH and titrate with a pK_a around 8.8, the pK_a of HONH-Ibm-Ala-GlyNH_2. Our observations are, of course, that K_{ass} *decreases* with increasing pH (Figure 2). There is clearly no hint of a pK_a near 9.

Temperature Dependence of Inhibition. The curved van't Hoff plot of Figure 3 indicates that the inhibition of TLN by HONH-Ibm-Ala-GlyNH_2 is a complex process that cannot be fully explained by a one-step mechanism. If the interaction of TLN and inhibitor obeyed a simple mechanism the temperature

(19) Hanguer, D. G.; Monzingo, A. F.; Matthews, B. W. *Biochemistry* **1984**, *23*, 5730–5741.
(20) Holden, H. M.; Matthews, B. W. *J. Biol. Chem.* **1988**, *263*, 3256–3265.
(21) Monzingo, A. F.; Matthews, B. W. *Biochemistry* **1984**, *23*, 5724–5729.
(22) Weaver, L. H.; Kester, W. R.; Matthews, B. W. *J. Mol. Biol.* **1977**, *114*, 119–132.
(23) Zalkin, A.; Forrester, J. D.; Templeton, D. H. *J. Am. Chem. Soc.* **1966**, *88*, 1804–1814.

Table II. Thermodynamic Parameters for the Association of Inhibitors or Substrates with Thermolysin[a] at 25 °C

inhibitor or substrate	ΔH_{ass} (kcal/mol)	ΔS_{ass} (eu)	$-T\Delta S_{ass}$ (kcal/mol)	ΔG_{ass} (kcal/mol)	$10^{-3}K_{ass}$[e] (M^{-1})
Z-Gly-Leu[b]	−5.2	−30	8.9	3.7	1.9
Z-Phe-GlyNH_2[c]	−6.7	−37	11	4.0	1.2
FA-Gly-Leu-Ala[d]	−7.9	−34	10	2.2	25
HONH-Ibm-Ala-GlyNH_2	−10.9	−31	9.2	−1.7	1,700

[a] All parameters were calculated with $[I]_{std\ state} = [S]_{std\ state} = 10^{-6}$ M and $T = 298$ K. [b] Parameters are from the work of Fukuda and Kunugi,[10] pH 6.5. [c] Parameters were calculated from the work of Kunugi and co-workers,[11] pH 6.6. [d] Parameters were taken from the work of Izquierdo and Stein[12] for K_s (*not* K_m) at pH 6.45. [e] $K_{ass} = (e^{-\Delta G/RT})/[I]_{std\ state}$.

dependence for K_{ass} would follow the straight, dashed line of Figure 3. This dependence is governed by the thermodynamic parameters $\Delta H = -11$ kcal/mol and $\Delta S = -31$ eu and predicts a monotonic rise in K_i from 18 to 600 nM over the temperature range of 5–60 °C.

The simplest mechanism that can account for our data is the two-step mechanism of Scheme I. While it may be tempting to equate the two steps of Scheme I with the two steps of Scheme IVB, it is clear that the second step of Scheme I occurs *after* formation of the final complex of Scheme IVB. That is, our analysis of the van't Hoff plot according to Scheme I indicates that, at temperatures less than 35 °C, $(E:I)_2$ does not accumulate and that inhibition is due entirely to accumulation of $(E:I)_1$ (see Figure 4). However, Scheme IVB states that the first complex never accumulates and that the stability of the final complex accounts for potent inhibition.

Thermodynamic parameters for the association of thermolysin with other ligands have been determined and are summarized, along with the results of this study, in Table II. The compounds in this table include three inhibitors, Z-Gly-Leu, Z-Phe-GlyNH_2, and HONH-Ibm-Ala-GlyNH_2, and a substrate, FA-Gly-Leu-Ala. Formation of $(E:I)_1$ is clearly enthalpy-driven: While ΔH_{ass} varies from −5 to −11 kcal/mol as inhibitor structure is varied, ΔS_{ass} is a constant at an average value of -33 ± 3 eu[24] ($-T\Delta S_{ass} = 10 \pm 1$ kcal/mol; $T = 298$ K). We believe that the dominant factor responsible for this decrease in ΔH_{ass} is increased affinity for the zinc, although hydrogen-bonding interactions between the ligands and TLN subsites must also make negative contributions to ΔH_{ass} and, thus, act to stabilize enzyme:inhibitor complexes. We also propose that ΔS_{ass} must reflect the cancellation of positive contributions from hydrophobic interactions of the inhibitor with the active site and the return of structured water to bulk solvent, by negative contributions that originate from the restriction of motion that accompanies coordination of the inhibitor to the zinc.

Finally, it is instructive to consider the curved van't Hoff plot for TLN inhibition in light of the curved Eyring plots that we previously reported for TLN catalysis.[12] In these latter cases, the data also suggested a multistep mechanism involving partial rate limitation by a physical step that follows the Michaels complex but precedes the chemical, catalytic step(s) involved in peptide bond hydrolysis. Taken together, these results suggest that thermolysin undergoes conformational isomerizations that are thermodynamically and kinetically significant and, thus, influence mechanistic details of both catalysis and inhibition.

(24) Much of ΔS_{ass} is a large entropy change that must be paid to simply bring together enzyme and inhibitor from our dilute standard state of 1 μM. At a standard state of 1 M, this entropy of "combination" has been estimated to be about −10 eu.[24,25] Thus, at a standard state of 1 μM, the entropy of combination equals −10 eu + R ln 10^{-6} = −37.6 eu (R ln 10^6 is a conversion factor, where R is the universal gas constant equal to 2 eu). We see then that if ΔS_{ass} is corrected for the entropy of combination of enzyme and inhibitor from dilute solution, the entropy change associated with formation of a stable E:I complex from an encounter complex is equal to −33 eu + 37.6 eu or 4.6 eu (1.4 kcal/mol at 298 °C).

(25) Jencks, W. P.; Page, M. I. *Proc. Eighth FEBS Meeting, Amsterdam* **1972**, *29*, 45–58.

(26) Page, M. I. *Angew. Chem., Int. Ed. Engl.* **1977**, *16*, 449–459.

Scheme V. Active, Exchangeable Protons in the Inhibition of TLN by HONH-Ibm-Ala-GlyNH_2

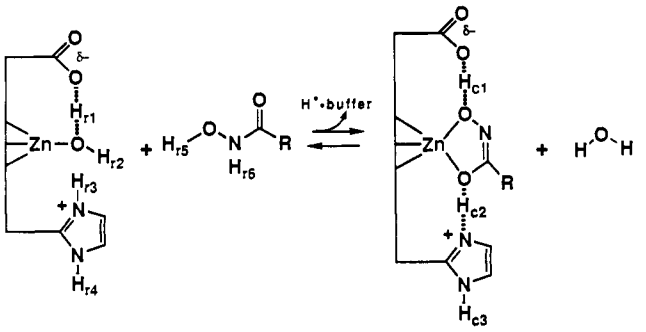

Solvent Isotope Effects on K_{ass}. The solvent deuterium isotope effect on K_{ass} for the inhibition of TLN by HONH-Ibm-Ala-GlyNH_2 is 0.74. Solvent isotope effects for equilibria processes are generally interpreted in the context of eq 11, where the effect is shown to be the ratio of products of fractionation factors for all exchangeable protons of the reactants and products, $\phi_{reactants}$ and $\phi_{products}$, respectively.[27]

$$^{D_2O}(K_{eq}) = \frac{\prod_{i=1}^{n}\phi_{reactants}}{\prod_{j=1}^{m}\phi_{products}} \qquad (11)$$

For the reaction under study here, our interpretation is aided by Scheme V, in which we show an abbreviated version of the inhibition mechanism of Scheme IVB and the exchangeable protons that may undergo a change in fractionation factor upon binding of inhibitor to enzyme and E:I complex formation. We assume that the other exchangeable protons of the enzyme and inhibitor have the same fractionation factor as in the E:I complex. Equation 11 can now be recast for the specific case at hand

$$^{D_2O}(K_{ass}) = \frac{\prod_{i=1}^{n}\phi_{ri}}{\prod_{j=1}^{m}\phi_{cj}} \qquad (12)$$

where ϕ_{ri} refers to protons of the enzyme and inhibitor reactants and ϕ_{cj} refers to the protons of the enzyme:inhibitor complex.

Thus, we can use eq 12 to calculate the isotope effect on K_{ass} by assigning values to ϕ_i and ϕ_j for each of the active protons of the reactants and enzyme:inhibitor complex. The most important of these fractionation factors are ϕ_{r1} and ϕ_{r2} (see Scheme V). Estimates for these fractionation factors can be found in a study of Co^{2+} carbonic anhydrases I and II[15] where an average value of 0.85 is reported for each of the two protons of H_2O–Co^{2+} and in a study of alcohol dehydrogenase[18] where, again, a value of 0.85 is reported for each of the two protons of H_2O–Zn^{2+}. This value will be used for both ϕ_{r1} and ϕ_{r2} in our calculation. If the fractionation factors for all the other exchangeable protons are assumed equal to unity,[27] we see that eq 12 simplifies to $^{D_2O}(K_{ass}) = (0.85)^2 = 0.72$. This value is in excellent agreement with our experimental value of 0.74.

It appears then that the solvent isotope effect on K_{ass} arises from transfer of the zinc-bound water, with $\phi_{r1} = \phi_{r2} = 0.85$, to bulk solvent, where by definition $\phi = 1$. We advanced this idea in previous publications to account for the solvent isotope effects of 0.74 on k_c/K_m for TLN-catalyzed peptide hydrolyses.[12,13]

In this study, we also found that the solvent isotope effect on K_{ass} does not vary with temperature. In the context of the mechanism suggested by the temperature dependence of K_{ass} (see Scheme I), this result suggests that, in both $(E:I)_1$ and $(E:I)_2$, the zinc-bound water has been transferred to bulk solvent. This supports the point we made earlier that $(E:I)_1$ cannot correspond

(27) Venkatasubban, K. S.; Schowen, R. L. *CRC Crit. Rev. Biochem.* **1985**, *17*, 1–41.

Scheme VI. Mechanism of Inhibition of Thermolysin by HONH-Ibm-Ala-GlyNH_2

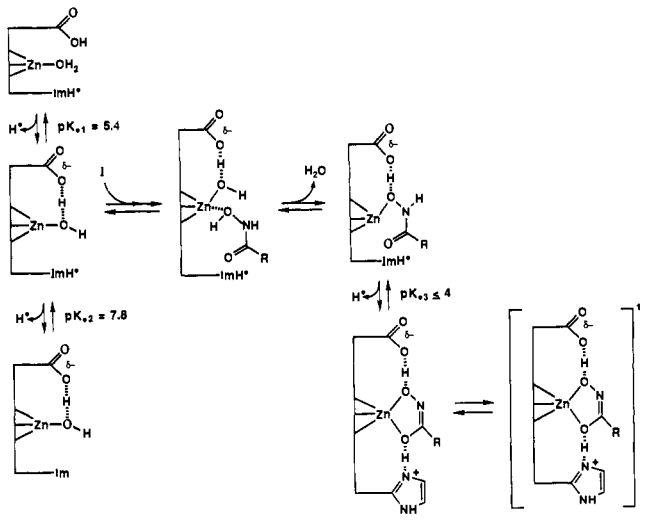

to an encounter complex in which both inhibitor and zinc-bound water are present in the active site.

Summary: Mechanism of Inhibition of Thermolysin by HONH-Ibm-Ala-GlyNH_2. The mechanism that we propose for the inhibition of thermolysin by the hydroxamic acid HONH-Ibm-Ala-GlyNH_2 is shown in Scheme VI. Essential features of this mechanism are as follows: (1) For productive complex formation with the inhibitor, thermolysin must be in the same ionization state that is required for catalysis. While we cannot rule out interaction of inhibitor with other ionized states of thermolysin, the initial complexes that result from these interactions will not be productive and go on to form stable complexes. Furthermore, it is the neutral, un-ionized form of the hydroxamic acid that binds to TLN, not the hydroxamate anion as suggested previously.[4-6] (2) Formation of the initial monodentate complex with displacement of the zinc-bound water molecule is a two-step process. This is required to avoid the energetically unfavorable mechanism involving dissociation of H_2O–ZnL_3 to ZnL_3 followed by complexation of inhibitor with ZnL_3. Thus, in the multistep reaction that we propose in Scheme VI, transfer of the zinc-bound water to bulk solvent occurs early on the pathway, prior to formation of stable complexes. (3) Formation of the stable bidentate complex is accompanied by ionization of the bound hydroxamic acid. This ionization is both necessary, since it is the anion of hydroxamic acids that interacts strongly with metal ions, and allowed, since at neutral pH the pK_a of the hydroxamic acid, like H_2O, will have been lowered upon interaction with the zinc. (4) At elevated temperatures, another complex accumulates. It is unclear what the structure of this complex is, but it may be a conformational isomer of the bidentate complex that is stable and accumulates at lower temperatures.

Acknowledgment. Thanks goes to Richard K. Harrison (Enzymology Department, Merck) for determining the pK_a of HONH-Ibm-Ala-GlyNH_2.

Characterization of the Structural Properties of α_1B, a Peptide Designed To Form a Four-Helix Bundle

John J. Osterhout, Jr.,[†] Tracy Handel,[‡] George Na,[§] Arazdordi Toumadje,[∥] Robert C. Long,[⊥] Peter J. Connolly,[†] Jeffrey C. Hoch,[†] W. Curtis Johnson, Jr.,[∥] David Live,*[,⊥] and William F. DeGrado*[,‡]

Contribution from the Central Research and Development Department, E. I. duPont de Nemours and Company, Experimental Station, Building 328, Wilmington, Delaware 1988-3028, The Rowland Institute for Science, 100 Cambridge Parkway, Cambridge, Massachusetts 02142, Sterling Research Group, 25 Great Valley Parkway, Malvern, Pennsylvania 19355, Department of Biochemistry and Biophysics, Oregon State University, Corvallis, Oregon 97331, and Department of Chemistry, Emory University, 1515 Pirece Drive, Atlanta, Georgia 30322.
Received March 8, 1991

Abstract: The structural and dynamic properties of α_1B, a peptide designed to self-associate into a four-helix bundle protein, have been examined using sedimentation equilibrium centrifugation, vacuum UV CD spectroscopy, and NMR spectroscopy. The peptide cooperatively forms tetramers, and the stability of the tetramer depends markedly on pH. CD and NMR spectroscopy indicate that the central core of the peptide is fully α-helical, and the N-terminal and C-terminal residues are structurally less well-defined. The NMR spectra are consistent with the symmetry of the designed tetramer and also suggest that the individual peptides in the tetramer dissociate to form monomers at rates that are intermediate to slow on the NMR time scale.

The mechanism by which proteins fold into their native, well-defined structures is a major, unsolved problem. One approach to the study of this problem involves the de novo design of proteins.[1-12] A rational strategy involves the design of sequences expected to display one of the basic motifs of protein structure (e.g., helix or sheet) and the evaluation of the correlation between the predicted and observed structural properties of these designs. Such sequences can then be elaborated into peptides and proteins that adopt supersecondary and tertiary structures with predictable structures and functions. Feedback from structural and functional studies plays an important role for iteratively improving the designs.

[†] The Rowland Institute.
[‡] DuPont.
[§] Sterling Research Group.
[∥] Oregon State University.
[⊥] Emory University.

(1) (a) DeGrado, W. F. *Adv. Protein Chem.* **1988**, *39*, 51-124. (b) DeGrado, W. F.; Wasserman, Z. R.; Lear, J. D. *Science* **1988**, *243*, 622-628.
(2) Gutte, B.; Däumigen, M.; Wittschieber, E. *Nature (London)* **1979**, *281*, 650-655.

0002-7863/92/1514-331$03.00/0